Coherent properties of super-continuum containing clearly defined solitons

Serguei M. Kobtsev and Serguei V. Smirnov

Novosibirsk State University, Pirogova 2, Novosibirsk 630090, Russia
kobtsev@lab.nsu.ru

Abstract: With the use of numerical simulations based on generalized nonlinear Schrödinger equation, we study for the first time the coherence of super-continuum (SC), generated in tapered and cobweb fibers in the regime with clearly defined solitions in spectrum. We suggest a simple model, which explains the influence of pump pulses power and duration on SC coherence. A possibility of concerned SC generation regime application in optical frequencies metrology is discussed.

OCIS codes: (190.0190) Nonlinear optics; (190.4370) Nonlinear optics, fibers

References and links

1. F. M. Mitschke and L. F. Mollenauer, "Discovery of the soliton self-frequency shift," Opt. Lett. **11**, 659-661 (1986).
2. K. L. Corwin, N. R. Newbury, J. M. Dudley, S. Coen, S. A. Diddams, B. R. Washburn, K. Weber, and R. S. Windeler, "Fundamental amplitude noise limitations to supercontinuum spectra generated in a microstructured fiber," Appl. Phys. B **77**, 269-277 (2003).
3. A. V. Husakou and J. Herrmann, "Supercontinuum generation of higher-order solitons by fission in photonic crystal fibers," Phys. Rev. Lett. **87**, 203901 (2001).
4. J. Herrmann, U. Griebner, N. Zhavoronkov, A. Husakou, D. Nickel, J. C. Knight, W. J. Wadsworth, P. St. J. Russell, and G. Korn, "Experimental evidence for supercontinuum generation by fission of higher-order solitons in photonic fibers," Phys. Rev. Lett. **88**, 173901 (2002).
5. A. Ortigossa-Blanch, J. C. Knight, and P. St. J. Russell, "Pulse breaking and supercontinuum generation with 200-fs pump pulses in PCF," J. Opt. Soc. Am. B **19**, 2567-2572 (2002).
6. W. J. Wadsworth, A. Ortigossa-Blanch, J. C. Knight, T. A. Birks, T.-P. M. Man, and P. St. J. Russell, "Supercontinuum generation in photonic crystal fibers and optical fiber tapers: a novel light source," J. Opt. Soc. Am. B. **19**, 2148-2155 (2002).
7. J. M. Dudley and S. Coen, "Coherence properties of supercontinuum spectra generated in photonic crystal and tapered optical fibers," Opt. Lett. **27**, 1180-1182 (2002).
8. J. M. Dudley and S. Coen, "Numerical simulations and coherence properties of supercontinuum generation in photonic crystal and tapered optical fibers," IEEE J. Sel. Top. Quantum. Electron. **8**, 651-659 (2002).
9. X. Gu, M. Kimmel, A. P. Shreenath, R. Trebino, J. M. Dudley, S. Coen, and R. S. Windeler, "Experimental studies of the coherence of microstructure-fiber supercontinuum," Opt. Express **11**, 2697-2703 (2003). http://www.opticsexpress.org/abstract.cfm?URI=OPEX-11-21-2697
10. J. Nicholson and M. Yan, "Cross-coherence measurements of supercontinua generated in highly-nonlinear, dispersion shifted fiber at 1550 nm," Opt. Express **12**, 679-688 (2004). http://www.opticsexpress.org/abstract.cfm?URI=OPEX-12-4-679
11. I. Zeylikovich, V. Kartazaev, and R. R. Alfano, "Spectral, temporal, and coherence properties of supercontinuum generation in microstructure fiber," J. Opt. Soc. Am. B **22**, 1453-1460 (2005).
12. S. M. Kobtsev, S. V. Kukarin, N. V. Fateev, and S. V. Smirnov, "Coherent, polarization and temporal properties of self-frequency shifted solitons generated in polarization-maintaining microstructured fibre," Appl. Phys. B **81**, 265-269 (2005).
13. G. P. Agrawal, *Nonlinear Fiber Optics* (Academic Press, San Diego, California, 2001).
14. K. J. Blow and D. Wood, "Theoretical description of transient stimulated Raman scattering in optical fibers," J. Quantum. Electron. **25**, 2665-2673 (1989).
15. S. M. Kobtsev, S. V. Kukarin, N. V. Fateev, and S. V. Smirnov, "Generation of self-frequency-shifted solitons in tapered fibers in the presence of femtosecond pumping," Laser Phys., **14**, 748-751 (2004).
16. B. R. Washburn, S. E. Ralph, P. A. Lacourt, J. M. Dudley, W. T. Rhodes, R. S. Windeler, and S. Coen, "Tunable near-infrared femtosecond soliton generation in photonic crystal fibres," Electron. Lett. **37**, 1510-1512 (2001).

#68698 - $15.00 USD Received 7 March 2006; revised 18 April 2006; accepted 18 April 2006

17. K. L. Corwin, N. R. Newbury, J. M. Dudley, S. Coen, S. A. Diddams, B. R. Washburn, K. Weber, and R. S. Windeler, "Fundamental amplitude noise limitations to supercontinuum spectra generated in a microstructured fiber," Appl. Phys. B **77**, 269-277 (2003).
18. S. Coen, A. H. L. Chau, R. Leonhardt, J. D. Harvey, J. C. Knight, W. J. Wadsworth, and P. St. J. Russell, "Supercontinuum generation by stimulated Raman scattering and parametric four-wave mixing in photonic crystal fibers," J. Opt. Soc. Am. B **19**, 753-764 (2002).
19. D. A. Jones, S. A. Diddams, J. K. Ranka, A. Stentz, R. S. Windeler, J. L. Hall, and S. T. Cundiff, "Carrier-envelope phase control of femtosecond mode-locked lasers and direct optical frequency synthesis," Science. **288**, 635-639 (2000).

1. Introduction

The effect of super-continuum generation by short light pulses passing through special optical fibres manifests itself in many ways. Super-continuum observed at the exit from an optical fibre may have diverse spectral and temporal structure, different polarisation, phase, noise, and other parameters, all of which may also be changing in the process of super-continuum development. One interesting variety of super-continuum realisation is generation of broad-bandwidth spectrally non-uniform radiation, the spectrum of which has strongly defined soliton structures in the long-wavelength wing (frequency self-shifted solitons [1]) and non-soliton radiation with relatively low spectral power density in the short-wavelength wing. This mode of generation is of great practical interest since solitons exiting the fibre may carry a significant fraction (several dozens of per cent) of the pump pulse energy, and their spectral position can be controlled by changing the power of pumping pulses. The longest- and the shortest-wavelength spectral components of such a super-continuum can be separated by more than an octave, and the intensity of generated frequency components may differ by several orders of magnitude [2] because of high spectral non-uniformity of radiation. In principle, this mode may be of interest for metrological applications, specifically for optical comb generators, however in order to understand the application prospects of this mode, particular attention should be paid to studying of phase and noise characteristics of solitons and the super-continuum radiation in the short-wavelength wing of the broad non-uniform spectrum.

The super-continuum generation mode that is characterized by the presence of only few well isolated solitons in the long-wavelength wing and by a broad short-wavelength wing of the radiation spectrum covering the wavelength range of several hundreds of nanometers has been studied in a number of publications (see, e.g., Ref. [3-6]), concentrated mainly on the spectral parameters of the radiation. In papers [3, 4], also the temporal distribution of intensity and spectral phase of SC was analyzed without consideration of coherent properties of radiation. In works [7-10] questions were discussed that touch upon coherent properties of SC containing strongly pronounced solitons in its spectrum, however the interplay of phase and noise radiation parameters in the long- and short-wavelength wings of such SC, as well as the dependence of coherent properties of radiation upon the spectrum width was not a special topic of study in these works. In paper [9], reciprocal coherence of SC generated inside two different fibres was investigated, which implies the presence of additional and stronger factors that destroy coherence as compared with the single-fibre case (the more traditional one from the viewpoint of SC generation techniques). Another special case was considered in Ref. [11] where fs pulses with wavelengths spaced by an octave (1560 and 780 nm) were used to generate SC. In Refs. [7, 8] the spectral, temporal, and coherent properties of SC were studied on the basis of the same numerical model as used in our work. The present paper is, in effect, a further development of these studies, as well as of Ref. [12], which is dedicated to experimental investigation of the coherence degree of different spectral components in SC containing well-isolated solitons in its spectrum. Discovered in Ref. [12] significant difference in coherent properties of spectral components of SC separated by an octave has given rise to the present numerical study of such SC in a broad range of pumping pulse parameters.

#68698 - $15.00 USD Received 7 March 2006; revised 18 April 2006; accepted 18 April 2006

Our distinction between super-continuum with strongly-pronounced soliton structures in the spectrum and that with unresolved solitons in the spectrum comes from the fact that well-isolated solitons typically have higher (or the highest) spectral density of the radiation power in comparison with other super-continuum components. Moreover, as it will be demonstrated further down, the spectral density of the radiation power in the central part of well-isolated soliton structures may be more than an order of magnitude higher than the average spectral power density of a flat-top (or quasi-flat-top) super-continuum with the same total energy and width of the super-continuum spectrum. When soliton structures overlap, the components of the long-wavelength super-continuum wing do not differ much from other super-continuum components in the spectral power density of radiation making such mode less interesting for applications, which aim at the use of components with the best parameters, such as the highest spectral density of radiation power and maximum degree of coherence. In the case of optical comb generators two octave-separated components of super-continuum spectrum are needed (f-to-2f interferometer), one of which may be located in the centre of a strongly isolated soliton structure.

In this work for the first time we investigate by way of numerical modelling the coherence of self-frequency-shifted solitons and of short-wavelength non-soliton radiation in order to find out optimal for applications generation modes of super-continuum with strongly pronounced soliton structures. Studied for the first time is the correspondence of soliton frequency shift and the degree of soliton coherence, also for the first time an analytical expression was derived that provides a relation between the duration and the power of pumping pulses that result in generation of SC with a fixed coherence degree. In the context of this research, the spectral and temporal parameters of such super-continuum are analyzed.

The super-continuum under consideration in the present paper is generated from femtosecond pumping pulses that propagate along a tapered or a cobweb fibre.

2. Numerical model

In the present work, for modelling of propagation of ultra-short laser pulses along an optical fibre the generalized non-linear Schrödinger equation was utilized [13]:

$$\frac{\partial A}{\partial z} = i\sum_{k=2}^{k_{\max}} \frac{i^k}{k!}\beta_k \frac{\partial^k A}{\partial t^k} + i\gamma\left(1+\frac{i}{\omega_0}\frac{\partial}{\partial t}\right)\left(A(z,t)\int_0^{\infty} R(t')\left|A(z,t-t')\right|^2 dt'\right) \qquad (1)$$

where $A(z, t)$ – the electric field intensity envelope, β_k – dispersion coefficients at the pump frequency ω_0, and $\gamma = n_2\omega_0/(A_{eff}c)$ – non-linear coefficient, where $n_2 = 3.2\text{x}10^{-20}$ m^2/W – non-linear refractive index of quartz and A_{eff} – effective cross-section area of the fundamental mode. The core $R(t)$ of the integral operator of the non-linear medium response was taken from the experiments referenced in Ref. [14]. It takes account of both electronic and vibrational (Raman) contributions.

Equation (1) can be derived without the use of slow-varying amplitude approximation [14], so that it is applicable for the description of propagation of pulses just a few light wave periods long at the corresponding frequency. When deriving Eq. (1) the assumption has been made that the radiation travels along the fibre in one (fundamental) mode. Besides, Eq. (1) is a scalar one and does not include polarisation effects. To solve Eq. (1) numerically we use Split-Step Fourier Method [13].

The first term in the right-hand side of Eq. (1), – the differential operator in time, – is responsible for the dispersion-induced evolution of pulses in the fibre. The term with $k = 2$ describes lengthening of Gaussian pulses and emergence of linear phase modulation as the pulses travel down the fibre; terms with $k > 2$ are responsible for higher-order dispersion effects which are important for femtosecond-range pulses, as they also are for longer pulses near the point of zero dispersion. In the conducted calculations expansion of the dispersion operator into a Taylor series in frequency was done up to the term with $k_{max} = 5$. The second

#68698 - $15.00 USD Received 7 March 2006; revised 18 April 2006; accepted 18 April 2006

term in the right-hand side of Eq. (1) takes into account a number of non-linear optical effects, such as four-wave mixing (FWM), self phase modulation (SPM), modulation instability (MI), self-steepening of the envelope wing and shock-wave formation, stimulated Raman scattering (SRS) [13]. Because of short (~10–20 cm) length of the fibres used in experiments and calculations Eq. (1) does not take into account linear losses that lead to exponential drop of the intensity as radiation travels along the fibre. Equation (1) also does not preserve energy because it includes the SRS effect. Instead, the invariant parameter in this equation is the number of photons [13, 14].

In studies of coherent properties of radiation propagated along an optical fibre, a superposition of signal and noise $A(0,t) = A_{signal}(t) + A_{noise}(t)$ is used as the initial condition when solving Eq. (1). Modelling of quantum noise is done by adding a single photon with a random phase in each of the mesh nodes in frequency representation, i.e. the absolute value of a complex quantity $A_{noise}(\omega)$ added to the amplitude of the spectral function is chosen according to the condition:

$$\left|A_{noise}(\omega)\right|^2 \cdot \Delta\omega = \hbar\omega \tag{2}$$

where $\Delta\omega$ – frequency interval between the nodes of the mesh on which the function $A(z,\omega)$ is defined. Functions $A(z,t)$ and $A(z,\omega)$ are related to each other through the Fourier transform. Laser pumping pulses were modeled in this work by use of spectral-limited sech^2 pulses, after their propagation through a linear medium with the second dispersion only $\tilde{\beta}(\omega) = \tilde{\beta}_2\omega^2/2$:

$$A_{signal}(t) = \int G(t,t')/\cosh(t'\cdot 2\ln(\sqrt{2}+1)/T_0)\,dt' \tag{3}$$

where Green function $G(t,t') = \int d\omega \exp\{i\tilde{\beta}(\omega)l - i\omega\cdot(t-t')\}/(2\pi)$, l – length of linear medium, T_0 – duration of spectral-limited pulses at half-maximum level. The phase of complex-valued function $A_{signal}(t)$ is nearly quadratic, i.e. $\arg A_{signal}(t) \approx Ct^2/(2T^2)$, where C – chirp parameter, T – duration of the pulse $|A_{signal}(t)|^2$ at half-maximum level. To characterize pumping pulses one should specify any two values of three (T_0, T, C).

Equation (1) allows one to describe successfully the effect of super-continuum generation and the soliton self frequency shift in optical fibres pumped with femtosecond pulses. Presented in Fig. 1 are typical spectra of self-frequency-shifted solitons obtained both in modelling and in experiment, in which 50-fs pulses at 805 nm were propagated through a 12-cm long bi-conical fibre with a 2.3-μm waist. The average power of pumping pulses was variable between 1.5 mW and 43 mW at the repetition rate of 81 MHz [15].

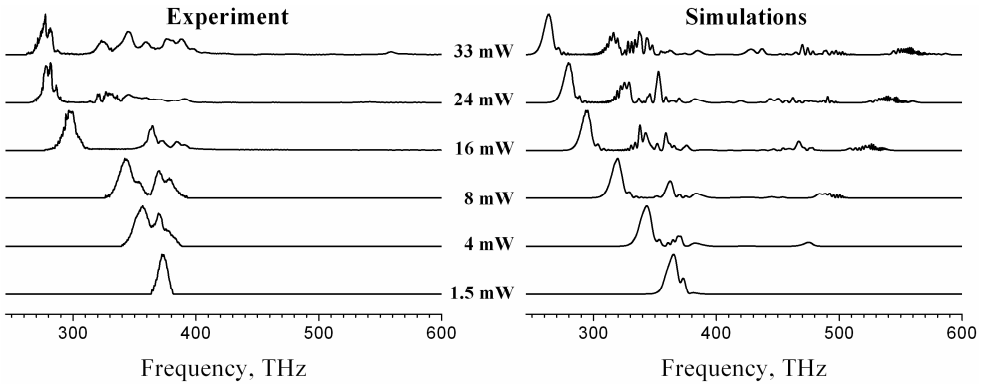

Fig. 1. Experimental (left) and calculated (right) radiation spectra at the exit from a bi-conical micro-waveguide at different average levels of pump power (corresponding values are given beside the curves).

#68698 - $15.00 USD Received 7 March 2006; revised 18 April 2006; accepted 18 April 2006

3. Results

The model we used earlier has demonstrated a good qualitative and quantitative (especially in the amount of soliton frequency shift) agreement of the modelling results with experimental data on bi-conical fibres (see Fig. 1 and Ref. [15]) and on photonic crystals [16], which is a fair ground to use this model for study of coherent properties of solitons. We have conducted calculations for typical bi-conical fibre (waist diameter 2.2 μm and 12-cm length) at different parameters of pump pulses with sech^2 envelope: peak power P, half-magnitude duration T_0 of initially spectrally limited sech^2-pulses and linear frequency modulation (chirp). Pumping pulse wavelength λ=805 nm (ω=373 THz), zero dispersion wavelength of the fibre λ_{ZD} = 740 nm (ω_{ZD} = 405 THz). In solving Eq. (1) we used the following values for dispersion coefficients of the fibre waist at the pump wavelength: $\beta_2 = -15.43$ ps^2/km, $\beta_3 = 8.447 \times 10^{-2}$ ps^3/km, $\beta_4 = -9.655 \times 10^{-5}$ ps^4/km, $\beta_5 = 1.888 \times 10^{-7}$ ps^5/km. Effective cross-section area of the fundamental mode was $A_{eff} = 3.188$ μm^2.

For each set of parameters for pumping pulses statistics was accumulated (100 calculations with random noise), upon which the dependence of the coherence degree on the frequency was derived:

$$g(\omega) = \frac{\left| \left\langle A_{(i)}(\omega) \cdot A^{*}_{(j)}(\omega) \right\rangle_{i \neq j} \right|}{\sqrt{\left\langle \left| A_{(i)}(\omega) \right|^2 \right\rangle_i \cdot \left\langle \left| A_{(j)}(\omega) \right|^2 \right\rangle_j}} \tag{4}$$

Here angular brackets are used for an average over the ensemble of spectral functions $A_{(i)}(\omega)$ generated as a result of independent computations for propagation of pumping pulses with random noise. Physically, the pair of functions $A_{(i)}(\omega)$ and $A_{(j)}(\omega)$ with $i \neq j$ may correspond both to two replicas of the single pumping pulse passing through different fibres and to two subsequent pumping pulses passing through the same fibre. However in the former case, as it was shown in Ref. [9], there are additional significant mechanisms of coherence degradation concerned with pump power fluctuations. The results of numerical modeling, presented in this paper, should be compared therefore with experiments, where the mutual coherence of successive pulses of SC, generated in single fiber, is measured.

The majority of dependencies $g(\omega)$ produced in calculations exhibit a fine structure — oscillations with ~1-GHz period. When the mesh size changed, as well as when the volume of sampling on which averaging is done in Eq. (4) increased, the fine structure was retained. Probably, oscillations of the $g(\omega)$ dependence are the result of the same mechanisms as is the fine structure in spectra. For convenient analysis of modelling results and their comparison with experiment, in which this fine structure may be unresolved both because of finite width of filter instrument functions and because of fluctuations of pumping pulse power, we give in this paper both graphs of $g(\omega)$ and smoothed dependencies obtained by convolution of $g(\omega)$ with a rectangle-shaped core having width $\Delta\omega$ = 2.5 THz ($\Delta\lambda$ ~ 5 nm in the vicinity of λ = 800 nm). Smoothed out dependencies are shown in the figures as bold solid lines, the original ones are drawn in thin gray lines. We plotted graphs of $g(\omega)$ at different values of the kernel width $\Delta\omega$ as well; as it was expected, larger $\Delta\omega$ leads to smoother dependencies, whereas smaller $\Delta\omega$ has the opposite effect. It should be especially noted that the soliton coherence, which is the focus of a detailed study in the work, practically does not depend on averaging because solitons do not contain fine structures either in spectra or in the $g(\omega)$ depencence.

On the left-hand side of Figs. 2(a)-2(c) a curve series is presented of calculated coherence degree *versus* radiation frequency for spectrally limited pumping pulses with power P = 15 kW and different half-magnitude duration ($T = T_0$ = 50, 75, 100 fs). For each value of pumping pulse duration there are two curves in Fig. 2: the dependence of coherence degree upon frequency $g(\omega)$ and the noise-averaged spectral power of radiation $I(\omega) = \langle |A_i(\omega)|^2 \rangle_i$,

#68698 - $15.00 USD Received 7 March 2006; revised 18 April 2006; accepted 18 April 2006

normalized to unity. Let's point out that for all calculations the results of which are given in Fig. 2 the pumping pulse power is sufficient to generate a high-order soliton that will, as it travels along the fibre, decompose into fundamental solitons. Thus, order N of the soliton at the fibre input is given by expression $N^2 = P/P_{fund}$, where $P_{fund} = |\beta_2|/(\gamma\tau^2)$ – peak power for the fundamental soliton, $\tau = T_0/1.76$. For P = 15 kW, T_0 = 50 fs we have P_{fund} ~ 244 W, N ~ 7.8, for T_0 = 75 fs we have P_{fund} ~ 109 W, N ~ 11.7, and for T_0 = 100 fs, P_{fund} ~ 61 W and N ~ 15.7. The given values of P_{fund} are applicable only for solitons at pumping power wavelength; for solitons at 1250 nm [that is the center wavelength of the soliton with maximum frequency shift in Fig. 2(c)] P_{fund} is about 15 times as high as for 805 nm due to the dependence of β_2 on frequency.

From the analysis of dependencies in Figs. 2(a)-2(c) it follows that the degree of coherence drops as pumping pulses grow longer. Thus, at T_0 = 50 fs [Fig. 2(a)] the degree of coherence is close to unity nearly over the whole spectrum. As the pulse duration increases to 75 fs [Fig. 2(b)], the radiation coherence is reduced throughout the spectrum leaving only isolated ~ 10-THz peaks with high coherence (g ~ 0.95). The degree of coherence at the frequency of 251 THz (λ = 1195 nm), corresponding to the intensity maximum of the longest-wavelength soliton in the spectrum, amounts only to g ~ 0.62. In the case T_0 = 100 fs, the coherence in most of the spectrum is lower than 0.10 – 0.15.

On the right-hand side of Figs. 2(a), 2(d), and 2(e), an analogous set of curves is shown for the case of positively-chirped pumping pulses (the frequency rises towards the trailing edge of the pulse). The duration T of the pumping pulses at half-magnitude and the chirp parameter C are specified to the right of the curves; the duration T_0 of spectrally limited pulses is constant in

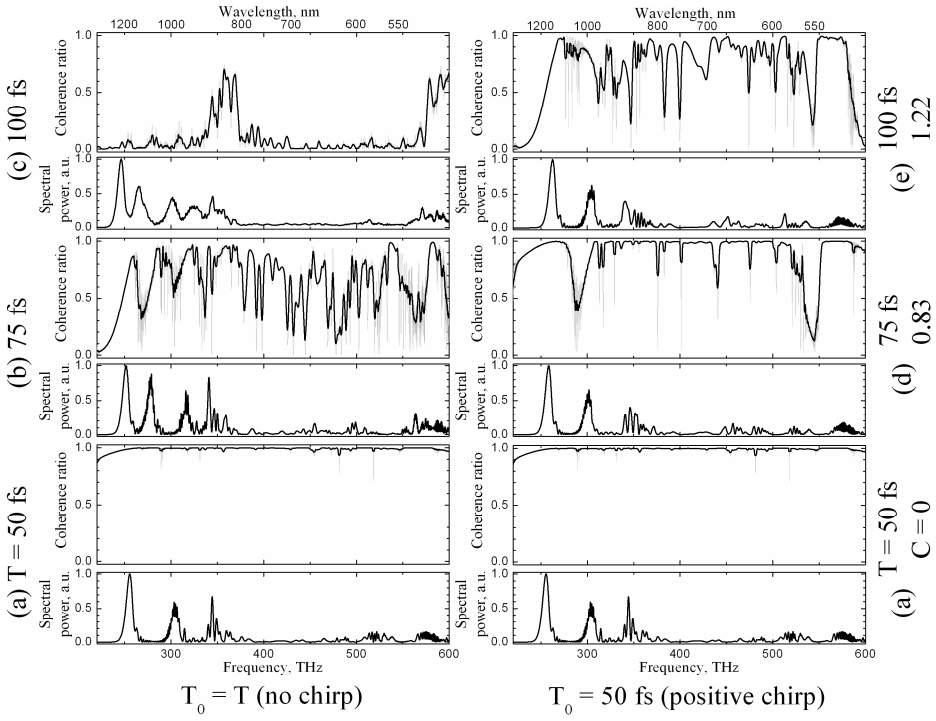

Fig. 2. Averaged over 100 computations dependence of coherence degree and spectral power at the exit from the waist of a bi-conical micro-waveguide (d = 2.2 μm, l = 12 cm) upon the radiation frequency at different values of input pulse duration. Pump pulse parameters: λ = 805 nm (ω = 373 THz), P = 15 kW; for graphs a–c: C = 0 (a–c), $T = T_0$ = 50 fs (a), 75 fs (b) 100 fs (c); for graphs d, e: T_0 = 50 fs (d, e), T = 75 fs, C = 0.83 (d), T = 100 fs, C = 1.22 (e).

#68698 - $15.00 USD Received 7 March 2006; revised 18 April 2006; accepted 18 April 2006

all cases and equals to 50 fs. It can be seen from the graphs that as the pump pulse duration increases the coherence of the radiation at the exit from the fibre becomes poorer because of the increase in linear frequency modulation (this conclusion is in agreement with other experimental and theoretical research of super-continuum noise: see, *e.g.*, Ref. [17]). The radiation coherence in this case happens to be noticeably higher than in the case of spectrally limited pumping pulses of the same duration, which is clearly visible when comparing curves in the left- and right-hand side columns of Fig. 2. These conclusions are also valid in respect of calculations with negative chirp of pumping pulses (corresponding curves are not presented in this paper).

Another computation series was carried out to study the dependence of the coherence degree of radiation passing through the fibre upon the pump power (Fig. 3). At P = 10 kW [Fig. 3(a)], the radiation coherence at the exit from a 12-cm fibre waist is close to unity almost over the entire spectrum with the exception of several frequencies around which function $g(\omega)$ has narrow and deep minima. The soliton in the long-wavelength part of the spectrum has frequency 265 THz (λ = 1132 nm) and coherence g = 0.96. As the power is raised to 15 kW [Fig. 3(b)], a further shift of the soliton into the long-wavelength range is observed to ω = 251 THz (λ = 1195 nm) and its coherence is reduced down to $g \sim 0.6$. Moreover, the coherence is also visibly lowered practically throughout the spectrum. When the peak pump power is further increased to 20 kW [Fig. 3(c)] the coherence continues to drop over the spectrum and, in particular, that of the soliton reaches $g = 0.1$ at ω = 240 THz (λ = 1250 nm). For all curves in Fig. 3 the peak power of the fundamental soliton with T_0 = 75 fs at the wavelength of the pump is P_{fund} = 109 W.

In addition to spectra and dependencies of coherence degree upon the frequency, presented in Fig. 3 are also temporal distributions of radiation intensity at the exit from the fibre generated in the same calculations [Figs. 3(d), 3(e), and 3(f)]. The correspondence between soliton peaks in the spectra and in the temporal distribution is indicated by numbers. According to what has been hitherto reported by other authors, from comparison of curves 3(a) and 3(d), 3(b) and 3(e), 3(c) and 3(f) in Fig. 3 one can see that the broad-band radiation of SC is a superposition of solitons and non-soliton radiation separated both in the spectrum and in time. At higher power of pumping pulses not only do solitons shift into the long-wavelength spectrum domain, but also become more widely separated in time. It is pertinent to note that as the pumping spectrum grows broader the temporal structure of radiation also becomes more complicated: more solitons are formed, they begin overlapping each other and the non-soliton radiation in time. It is clearly visible in Figs. 3(e), and 3(f) at values of t between 0 and 1 ps because wavelengths of SC components falling into this interval are close to λ_{ZD} and therefore these spectral components have similar group velocities. Calculations show that solitons in the long-wavelength spectrum wing have duration $T_0 \sim 45$ fs and their peak power is close to the power of fundamental soltions at the corresponding frequency and specified dispersion coefficients β_k. Since the conclusions arrived at are equally valid for other calculations, the results of which are presented in this paper, we limited ourselves to giving the temporal intensity distributions in Fig. 3 only.

It is interesting as well to follow the evolution of the coherence degree as the pumping pulse travels down the fibre (see Fig. 4). At z = 0 [Fig. 4(a)] the coherence in the vicinity of pump frequency equals 1. The width of the region where g=1 spans about 35 THz (the width of the pumping pulse spectrum at half-magnitude being ~ 4.5 THz) and is defined by the condition $|A(0,\omega)| >> |A_{noise}(\omega)|$, where the noise level in the pump radiation is given by Eq. (2). Outside this frequency range the coherence degree extracted from calculations is at the level of ~ 0.01; its difference from zero rises from the finite sampling volume over which averaging is done in Eq. (4).

#68698 - $15.00 USD Received 7 March 2006; revised 18 April 2006; accepted 18 April 2006

As the pump radiation travels along the fibre, its spectrum is extended both into longer wavelengths (owing to the effect of self frequency shift of solitons) and into the short-wavelength domain. At the same time a gradual reduction of the coherence degree over the entire spectrum takes place. For instance, at z = 6 cm a soliton in the long-wavelength part of the spectrum is shfted down to 272 THz (λ = 1100 nm), its degree of coherence being ~ 0.97. Radiation in the short-wavelength part from 550 to 615 THz is also highly coherent: g ~ 0.95 – 0.98 [see Fig. 4(c)]. At z = 9 cm the carrier frequency of the soliton drops to 259 THz (λ = 1160 nm), g ~ 0.84. At z = 12 cm its frequency ω_{sol} = 251 THz (λ = 1195 nm), g ~ 0.6.

#68698 - $15.00 USD Received 7 March 2006; revised 18 April 2006; accepted 18 April 2006

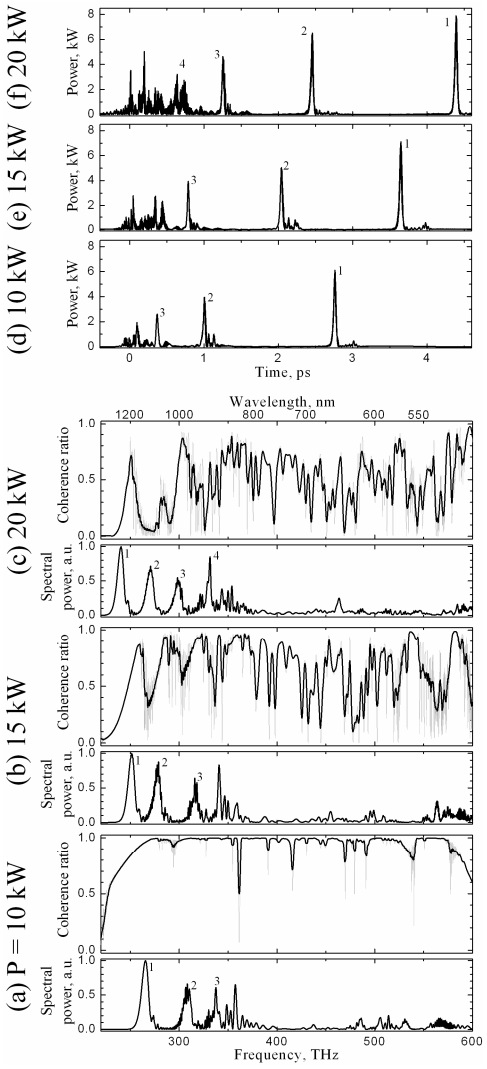

Figs. 3. (a), (b), and (c) averaged over 100 calculations dependence of coherence degree and spectral power at the exit from the waist of a bi-conical micro-waveguide (d = 2.2 μm, l = 12 cm) on the radiation frequency at different power levels of input pulses. Parameters of pumping pulses: λ = 805 nm (ω = 373 THz), $T = T_0$ = 75 fs (C = 0), P_{fund} = 109 W, P = 10 kW(a), 15 kW(b), 20 kW (c). (d), (e), (f) – temporal intensity distributions at the exit of the fiber for the same simulations.

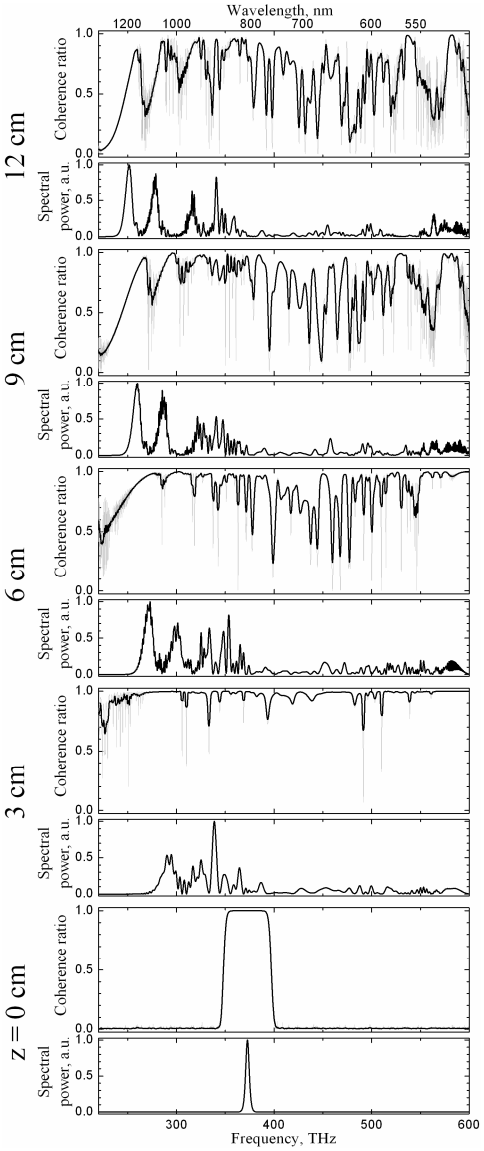

Fig. 4. Dependence of the coherence degree and spectral power on the radiation frequency upon the pumping pulse passing distance z = 0 (a), 3 cm (b), 6 cm (c), 9 cm (d), and 12 cm (e) along the waist of a bi-conical micro-waveguide (d = 2.2 μm, l = 12 cm). Pump parameters: λ = 805 nm (ω = 373 THz), P = 15 kW (P_{fund} = 109 W), $T = T_0$ = 75 fs.

It can be seen from the figures discussed earlier that the broadening of the radiation spectrum is accompanied with reduction of its degree of coherence. Therefore, one of the

#68698 - $15.00 USD Received 7 March 2006; revised 18 April 2006; accepted 18 April 2006

problems in optimization of continuum generators or generators of self-frequency-shifted solitons for applications may consist in search for conditions under which the broadest spectrum (soliton frequency shift) can be produced while maintaining the highest possible degree of coherence. In order to solve the presented problem let us refer to Fig. 5 in which dependencies are given of the coherence degree upon the frequency shift of the longest-wavelength soliton. Calculations were performed for three values of the peak power of the pumping pulses (shown with markers of different shape) and for different durations (the corresponding values are given beside the graph points). Curves (a), (b), (c) in Fig. 5 differ in the distance covered by the pumping pulse along the fibre waist with diameter 2.2 μm. The curves demonstrate that as the duration of pumping pulses, their power, and the distance travelled along the fibre grows, the shift of the soliton carrier frequency increases and soliton coherence drops.

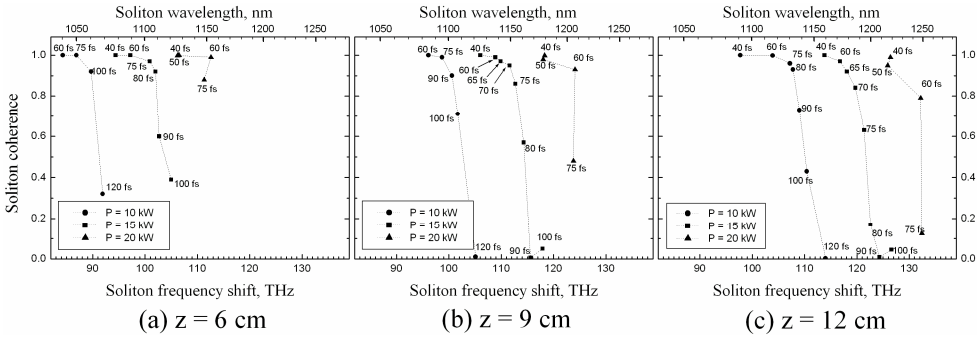

Fig. 5. Dependence of the coherence degree of the longest-wavelength soliton in the spectrum upon the frequency shift. Calculations were carried out for the fibre waist diameter 2.2 μm and waist length 6 cm (a), 9 cm (b), 12 cm (c). Duration and power of pumping pulses are given in the graphs.

In order to increase the frequency shift of the soliton while maintaining high coherence of radiation it is necessary to use the shortest possible pumping pulses, longer fibre and higher pumping power. For example, when 40-fs pumping pulses are used the radiation remains coherent throughout the spectrum even at maximum values of the pump power and fibre length covered in the study (P = 20 kW, z = 12 cm). When pumping with 75-fs pulses, the power should be lowered to 10 kW, at which value the coherence of the longest-wavelength soliton in the spectrum will amount to $g \sim 0.96$ (z = 12 cm) and to $g > 0.99$ (z = 9 cm).

When analysing the dependencies presented above and choosing the optimal parameters for the generation of super-continuum with given properties it is necessary to bear in mind that the model used in computations contains at least one “free” parameter that cannot be measured directly in an experiment. This parameter is the size of the mesh on which the numerical solution $A(z,\omega)$ of Eq. (1) is sought. The mesh size $\Delta\omega$ is not a physical parameter characterizing a real experiment and, therefore, one would reasonably expect independence of the calculation results of $\Delta\omega$, on the condition that it is chosen correctly (lies within certain limits). However, this is not the case because the value of $\Delta\omega$ enters Eq. (2) that determines the normalization of the noise magnitude in the pump radiation. And the level of random noise at the entrance into the fibre affects the degree of radiation coherence at the fibre exit. So, if the noise level is increased ten-fold the coherence of the longest-wavelength soliton in the spectrum drops from 0.97 to 0.75 (computation parameters: P = 15 kW, $T = T_0$ = 60 fs, z = 12 cm). The meaning of parameter $\Delta\omega$ is analogous to that of the normalization volume in quantum mechanics ($L = 2\pi c/\Delta\omega$), which arises, for instance, when the energy of the blackbody radiation is calculated or electro-magnetic field is quantized. If, instead of Eq. (2), one uses a different noise normalization condition independent of $\Delta\omega$ the calculation results, as is to be expected, cease to depend on the mesh size. The requirement of noise normalization

#68698 - $15.00 USD Received 7 March 2006; revised 18 April 2006; accepted 18 April 2006

(and the following from this presence of a free parameter) is caused directly by a phenomenological description of noise. In spite of the fact, this model was already successfully used for description of SC generation [18], specifically for study of noise in the SC radiation [2, 7, 8].

4. Discussion

The results presented earlier, which were produced in the numerical modelling, admit the following qualitative explanation. At the start of pump pulse propagation along the fibre one clearly sees amplification of noise on both sides of the pump line that is caused by MI. The maximum of the power gain coefficient g_{max} is reached at frequencies $\omega_0 \pm \Omega_{MI}$ [13], where

$$\Omega_{MI} = \sqrt{\frac{2\gamma P}{-\beta_2}}, \quad g_{\max} = 2\gamma P \tag{5}$$

Instability develops until the spectral power of noise in the maxima of the gain contour is equal by order of magnitude to the spectral power of the pumping pulse. The fibre length necessary for it is

$$z_{MI} \approx \frac{1}{2\gamma P} \cdot \ln \frac{I_0}{I_{noise}} \tag{6}$$

(here I_0 and I_{noise} – spectral power of pump in the centre of the line and of noise at the entrance into the fibre respectively). The coherence of radiation generated in MI lines will be zero since these spectral components emerged because of noise amplification and hence have random phase. As the radiation travels further along the fibre its spectrum width will grow because of FWM and SRS, whereas its coherence will decrease over the whole spectrum as z increases because of MI noise that has random phase.

Despite the line shape and the gain factor of MI are independent of the duration of the pump pulses T_0, the spectral broadening scenario just explained is only valid for sufficiently long pulses. As T_0 grows lower (or as power P increases), another effect comes into play, which is given rise to by Kerr non-linearity — SPM. A phase shift caused by this effect leads to the broadening of the pumping line by a factor, which has the order of magnitude [13]:

$$\delta\omega(z) = k \cdot \frac{\gamma P z}{T_0} \tag{7}$$

(This expression was derived under fairly rough approximation of constant peak power of the pump radiation in the beginning of propagation along the fibre; coefficient k for Gaussian pulses amounts to a value in the vicinity of 1.43). In case the radiation spectrum width broadens to $2\Omega_{MI}$ because of SPM as the radiation propagates to a point $z_{SPM} < z_{MI}$ the broadened pump spectrum will overlap with MI gain lines, which will lead to a rapid growth of instability and decay of the pulse. A broadband radiation generated as a result must be completely coherent in the limit of $z_{SPM} << z_{MI}$, because in this case it is generated from amplification of stable pump radiation components and not from random noise.

Between the two limits we have considered one may expect a dependence of the coherence degree g on z and on ratio $\xi = z_{MI}/z_{SPM}$ that characterizes relative contribution of random noise amplified by MI and that of stable spectral components of pump radiation into the generated broad-band radiation. Solving equation $\delta\omega(z_{SPM}) = \Omega_{MI}$ for z_{SPM} and using Eq. (5), Eq. (6), and Eq. (7) we have

$$\xi = \sqrt{\frac{-\beta_2 \cdot k^2}{8T_0^2 \gamma P}} \cdot \ln \frac{I_0}{I_{noise}} \tag{8}$$

#68698 - $15.00 USD Received 7 March 2006; revised 18 April 2006; accepted 18 April 2006

Thus, we have derived that

$$g(P, T_0, z) = g(PT_0^2, z) \tag{9}$$

That is, the degree of coherence must depend on the power and pulse duration of the pump only through combination PT_0^2. Dependencies of soliton coherence on P and T_0 at z = 6, 9, 12 cm shown in Fig. 5 allow one to assert the agreement between the results of the simple argument given above and the modelling results, thus proving the validity of suggested mechanism of coherence decay. For instance, at z = 6 cm the value of g(100 fs, 10 kW) must equal g(82 fs, 15 kW) and g(71 fs, 20 kW) — the results of calculation show that g(100 fs, 10 kW) = g(80 fs, 15 kW) = 0.92, g(75 fs, 20 kW) = 0.88. At z = 9 cm the same equalities only hold to the precision of about 20%, which may be explained by an error in g definition: in Fig. 2 it is visible that $g(\omega)$ may change widely within a single soliton (specifically, for T_0 = 75 fs, P = 15 kW, z = 12 cm $0.27 < g(\omega) < 0.87$). The same fact may be accountable for a better correspondence of Eq. (9) to the computation results in case when coherence is near 1 or 0, because under this condition the spread of $g(\omega)$ values within one soliton is insignificant.

5. Conclusion

The effect of self frequency shift of solitons presents a serious practical interest, first of all because it may be used in development of universal sources of short-pulsed coherent radiation with wavelength tuning by adjustment of pump power. Such sources may be in demand for a number of application fields: spectroscopy, optical tomography, and others. Optical clock is one important and prospective application of super-continuum containing strongly pronounced soliton structures, as it was noted in the Introduction. This application poses two major conditions on the generated radiation. First, the spectrum of the comb generator must be composed of equidistant set of lines with $\omega_n = n f + \omega_c$, intervals f between which are equal to the repetition frequency of the pumping pulses, and the frequency shift ω_c arises as a result of difference between the average values of group and phase velocities inside the pump laser. This difference leads to a phase difference between two successive pumping pulses. Second, the super-continuum spectrum should at least cover an octave, *i.e.* include lines ω_n and ω_{2n} that lie both in the optical range [19]. These conditions may be satisfied not only by a broad continuum with a flat spectrum traditionally considered in the context of this problem. They may also be satisfied by a broad-band spectrally non-uniform frequency continuum that includes self frequency shifted solitons together with short-wavelength non-soliton radiation. As the calculations discussed above demonstrate the radiation of frequencies of such super-continuum separated by an octave may be coherent, and a spectrum that fulfils these conditions may be produced, in particular, at P = 10 kW, T_0 = 50 fs, z = 9 cm. The power of radiation at frequency ω_{2n} equal, for instance, to 560 THz will be approximately 5% higher than the corresponding level for frequency continuum with the same pulse energy and flat-top spectrum covering the range between ω_n and ω_{2n}. In this case the spectral power at frequency ω_n = 280 THz (corresponding to the soliton with maximal frequency shift that contains more than 40% of the pulse energy) turns out to be ten times higher than the spectral power of continuum with flat-top spectrum, which presents a possibility of registering beats between frequencies $2\omega_n$ and ω_{2n} and improves substantially the precision of referencing of the pump laser frequency to the continuum frequency ω_n because of its relatively high intensity. Thus, the results of numerical modelling suggest that a super-continuum characterized by strongly pronounced soliton structures in the long-wavelength wing of its spectrum and by non-soliton radiation with relatively low spectral power density in the short-wavelength wing can be efficiently used in optical clock applications.

#68698 - $15.00 USD Received 7 March 2006; revised 18 April 2006; accepted 18 April 2006

Acknowledgments

This work was supported by the INTAS, project No. 03-51-5288.

#68698 - $15.00 USD Received 7 March 2006; revised 18 April 2006; accepted 18 April 2006